Amazonian-aged fluvial valley systems in a climatic microenvironment on Mars: Melting of ice deposits on the interior of Lyot Crater

J. L. Dickson,[1] C. I. Fassett,[1] and J. W. Head[1]

[1] Valley networks, regional drainage patterns suggesting liquid water stability at the surface, are confined to early in the history of Mars (the Noachian/Hesperian boundary and before), prior to a major climate transition to the hyperarid cold conditions of the Amazonian. Several later fluvial valley systems have been documented in specific Hesperian and Early Amazonian environments, and are thought to have formed due to local conditions. Here we describe fluvial valley systems within Lyot crater that have the youngest well-constrained age reported to date (Middle or Late Amazonian) for systems of this size (tens of km). These valleys are linked to melting of near-surface ice-rich units, extend up to ∼50 km in length, follow topographic gradients, and deposit fans. The interior of Lyot crater is an optimal micro-environment, since its low elevation leads to high surface pressure, and temperature conditions at its location in the northern mid-latitudes are sufficient for melting during periods of high-obliquity. This micro-environment in Lyot apparently allowed melting of surface ice and the formation of the youngest fluvial valley systems of this scale yet observed on Mars. **Citation:** Dickson, J. L., C. I. Fassett, and J. W. Head (2009), Amazonian-aged fluvial valley systems in a climatic microenvironment on Mars: Melting of ice deposits on the interior of Lyot Crater, *Geophys. Res. Lett.*, *36*, L08201, doi:10.1029/2009GL037472.

1. Introduction

[2] Valley networks [*Carr*, 1996] and the mineralogy [*Bibring et al.*, 2005] of the Martian highlands respectively demonstrate that periods of fluvial erosion and aqueous alteration occurred on Mars in the Noachian, a period likely characterized by a warmer and wetter climate. Limited fluvial activity extended into the Hesperian and Early Amazonian [e.g. *Gulick and Baker*, 1990; *Mangold et al.*, 2004; *Fassett and Head*, 2008], but these are likely due to localized environments, rather than to a continuation of the Noachian climate. No fluvial valley systems at the scale of tens of kilometers have yet been reported during the Middle to Late Amazonian.

[3] The Middle/Late Amazonian climate is interpreted to have been much the same as that of today: a cold hyperarid desert [*Marchant and Head*, 2007] with average conditions below the triple point of water. Ice is not stable at the surface in equatorial and mid-latitude regions [*Mellon and Jakosky*, 1995], but due to variations in spin-axis/orbital parameters [*Laskar et al.*, 2004], ice during the Late Amazonian was mobilized from high-latitudes and re-deposited equatorward as interpreted from: 1) remnants of tropical mountain cold-based glaciers [*Head and Marchant*, 2003]; 2) mid-latitude glacial deposits [e.g., *Holt et al.*, 2008, and references therein]; and 3) latitude-dependent mantling deposits from ∼30° latitude to the poles interpreted to be remnants of a recent ice age [*Mustard et al.*, 2001; *Head et al.*, 2003].

[4] In spite of the fact that the Middle and Late Amazonian climate of Mars has generally been below the triple point, analyses of the global topography and atmosphere show that some areas on Mars are characterized by micro-environments within which liquid water is stable on the surface for short periods of time (tens of days) throughout the Martian year [*Haberle et al.*, 2001; *Lobitz et al.*, 2001]. This prompted us to investigate the most likely micro-environments that might have permitted melting of surface/near-surface ice, especially impact craters at low elevations in the mid-latitudes, which provide high pressure and high insolation under optimal climate conditions.

[5] Lyot Crater, a ∼215 km basin in the northern low-lands (50°N, 30°E) (Figure 1a) fits these constraints. With a floor elevation of ∼ −7000 m, Lyot represents the lowest point in the northern hemisphere. *Haberle et al.* [2001] calculated a maximum surface pressure at Lyot of >10 mb, above the triple point of water (6.1 mb), consistent with the calculations of *Lobitz et al.* [2001]. Stratigraphy shows that Lyot formed in the Early Amazonian [*Greeley and Guest*, 1987], post-dating the cessation of extensive valley network development [*Fassett and Head*, 2008].

[6] Lyot is north of Deuteronilus Mensae (Figure 1a), an area characterized by Lineated Valley Fill (LVF) and Lobate Debris Aprons (LDA), interpreted to represent networks of glacial flow [*Head et al.*, 2006a, 2006b]. Analysis of these deposits suggests past ice thicknesses of ∼1 km [*Dickson et al.*, 2008]. Given the youth of Lyot, its proximity to Amazonian glacial deposits, and its unusually high surface pressure, we used high-resolution data to examine the Lyot micro-environment for evidence of ice-rich deposits and liquid water.

2. Observations

2.1. Lyot Crater Interior

[7] At Context Camera (CTX) resolution (∼6 m/px), a mantling unit blankets the majority of Lyot and adjacent plains (Figure 1b). This unit has a stippled texture (Figures 2 and 3), diffuse margins, and impacts within the unit range from fresh bowl-shaped craters to rimless depressions. Three CTX frames of the eastern portion of Lyot permitted us to map this unit in detail (Figure 1b).

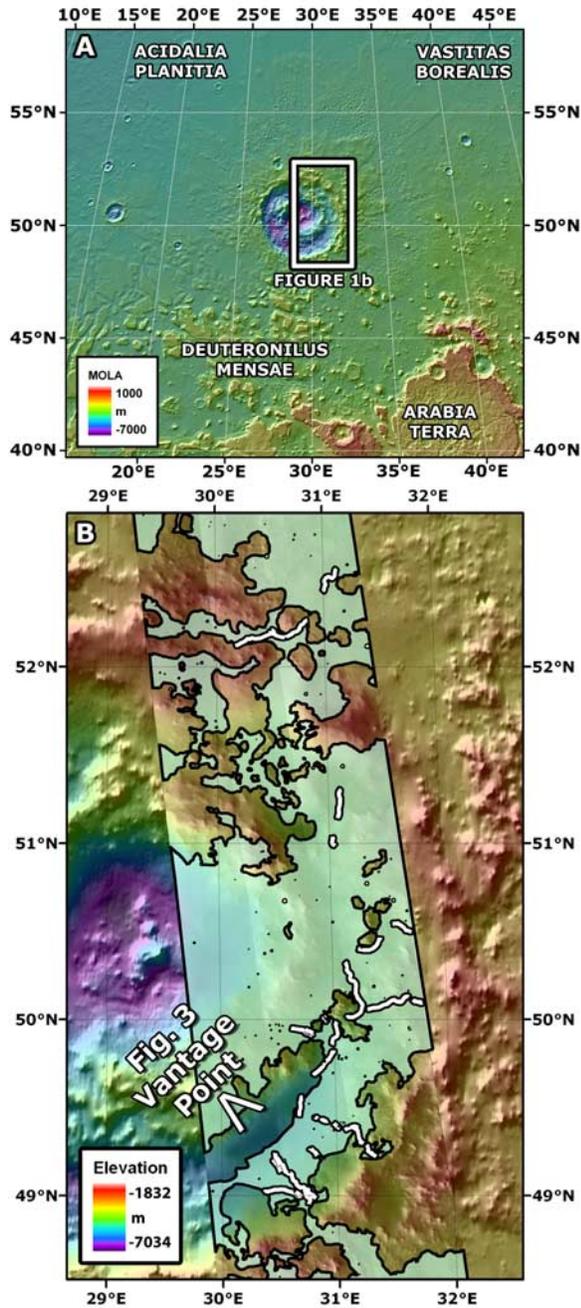[1]Department of Geological Sciences, Brown University, Providence, Rhode Island, USA.

Figure 1. (a) Lyot Crater. MOLA topography over shaded relief. Lyot ejecta superposes Amazonian plains to the north (*Aps* in the work by *Greeley and Guest* [1987]). Deuteronilus Mensae has been modified by extensive Amazonian glaciation [*Head et al.*, 2006a, 2006b]. (b) Distribution of (1) stippled mantling unit (green); (2) fluvial valley systems (white); and (3) impact craters mapped within the stippled mantling unit (small circles mapping their true extent). Detailed mapping limited to CTX availability.

[8] Along the Lyot rim and peak ring, deposits similar to glacial features mapped in Deuteronilus Mensae [*Head et al.*, 2006a, 2006b] are observed (Figure 3). These features contain convex-outward ridges, convex-upward profiles, and features indicative of debris-covered glacier deposits [e.g. *Head et al.*, 2005, 2006a, 2006b] (Figure 3). They are prominently observed along the southern interior rim, where three LDAs extend from the rim towards the floor (Figure 3). Knobs along the rim and peak ring also host LDAs, as well as young gully systems [*Hart et al.*, 2008].

2.2. Fluvial Valley Systems

[9] The interior of Lyot exhibits several systems of sinuous valleys incised into the stippled mantling unit. Twenty systems are observed, fifteen of which occur in the eastern half of Lyot (Figure 1b). Valleys range in length from 2–50 km with widths that average ∼250 m. They follow local gradients (Figure 3), with slopes in the down-valley direction ranging from 0.4° to 6° (median = 2°). Valleys start at a range of elevations in the crater interior, from ∼−2880 m to ∼−5680 m (mean = −3800 m). Valley walls appear sharp and no impact craters are observed on valley floors (Figure 2). Valleys are superposed by smooth material on the flanks of isolated mesas where the two units are found in conjunction (Figure 2b).

[10] Several of the longer valleys deposit alluvial fans at their termini (Figures 2c and 2d). These deposits show a range in morphology from fans with broad, smooth surfaces (Figure 2c) to smaller dissected examples (Figure 2d). The largest valleys in Lyot produced the largest fans, as observed in Figure 2c, which shows a fan emanating from a 28 km valley on the northern rim of Lyot. This fan exhibits a 2.9° scarp, based upon MOLA altimetry tracks, and these data suggests a thickness of ∼60 m.

[11] The dissection and modification of many of the smaller fans in Lyot (e.g., Figure 2d) appears to have been unrelated to valley activity, suggesting that modification has taken place over a significant period of time. Nonetheless, the existence of these fans in Lyot, comparable in size and morphology to alluvial fans on the Earth and Mars, as well as the low slopes and meandering nature of the valleys, supports the interpretation that the valleys were carved by fluvial processes.

3. Chronology

[12] Crater size-frequency distribution measurements of Lyot and its ejecta using High Resolution Stereo Camera (HRSC) data yield a formation age for Lyot of Early Amazonian for both the *Neukum* [*Ivanov*, 2001] (∼3.3 Gyr) and *Hartmann* [*Hartmann*, 2005] (∼1.6 Gyr) isochron systems (Figure 4a). Stratigraphic relationships are consistent with an Early Amazonian age as well, as Lyot ejecta superposes Amazonian smooth plains material (*Aps* in the work by *Greeley and Guest* [1987]). These constraints show that Lyot formed well after the cessation of ancient valley network activity [*Fassett and Head*, 2008].

[13] We interpret the fluvial valley systems of Lyot to have incised the stippled mantling unit. We performed crater counts on this unit to obtain a maximum age for valley network formation. Due to resolution and spatial footprint constraints, we focused our mapping on the three CTX orbits in eastern Lyot (Figure 1b), where the majority of valley systems are observed. The subdued morphology of craters within this unit makes superposition relationships unclear in some cases; thus we counted every crater
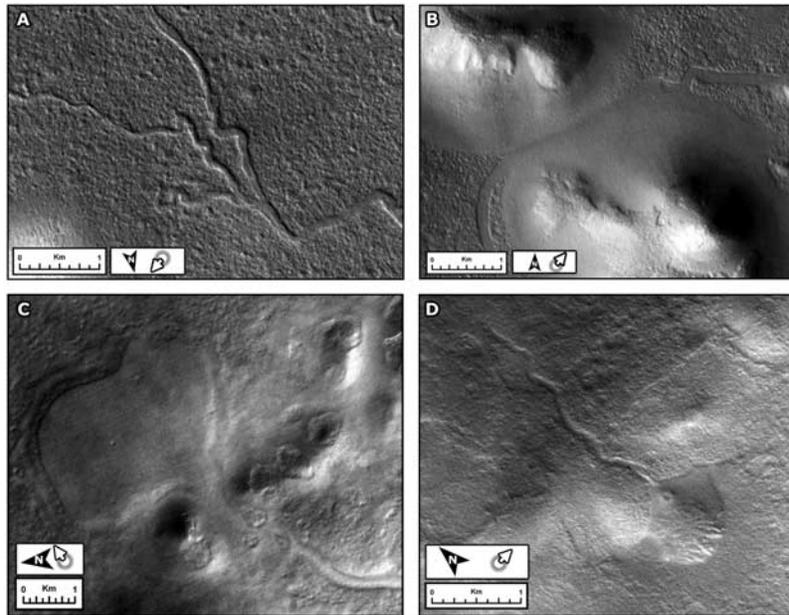
Figure 2. Lyot crater fluvial valley systems and fans. (a) Valleys converging and trending downslope toward the lower right (CTX P04_002560_2309), (b) Smooth mantling deposits on knobs superposed on valleys. Direction of flow from topography was from upper-right to lower-left (CTX P04_002560_2309). (c) Broad fan sourced by a ~28 km valley (CTX P04_002494_2310). (d) Smaller dissected fan sourced by small channel from the north (CTX P04_002494_2310).

observed within the unit, providing a conservative maximum age.

[14] We calculated a Middle Amazonian age for the stippled mantling unit, with a best fit of ~1.5 Gyr in the *Neukum* [*Ivanov*, 2001] system and 0.78 Gyr in the *Hartmann* [*Hartmann*, 2005] system. This measurement is well matched by production model isochrons (Figure 4b) and is consistent with stratigraphic constraints. Thus, we are confident that these valleys are Middle Amazonian or younger. There is a substantial (0.8–1.9 Gy) period of time between the Lyot impact and the emplacement of the stippled mantling unit, suggesting that valley formation significantly post-dates the formation of Lyot.

4. Discussion

[15] Like the Noachian-aged valley networks, the fluvial valley systems of Lyot display morphologies (Figure 2) and topographic relationships typical of fluvial features carved by liquid water, but at a much younger time (Figure 4). What is the source of the water? We propose that the glacial deposits found within Lyot and the stippled mantling unit itself provide the most plausible sources (Figure 3). We interpret the direct association of debris-covered glacial deposits and these fluvial valley systems (Figure 3) as evidence of cause and effect, and suggest that the glaciers were a significant source of meltwater for these valley systems (Figure 2a).

[16] What processes could have provided enough energy for melting of these ice-rich deposits? While the Lyot impact likely initiated groundwater convection that delivered energy to the surface, the time span between impact and emplacement of the stippled mantling unit (at least 800 Myr (Figure 4)) surpasses the greatest model lifetimes for impact-induced thermal anomalies in terrestrial
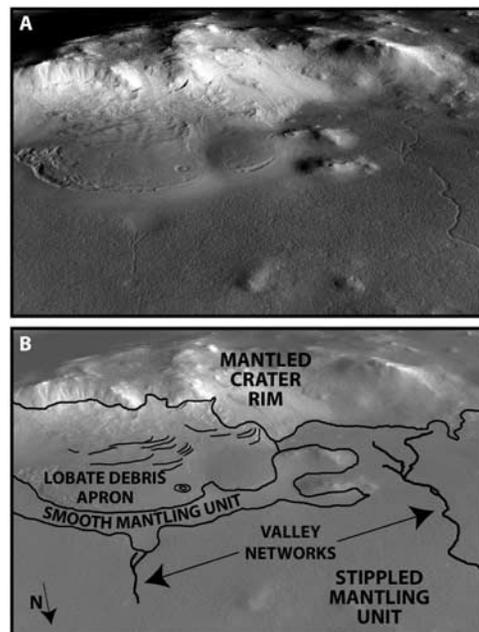

Figure 3. (a) Perspective view of the southern Lyot rim. (b) Sketch map overlain on identical perspective view. We observe (1) a broad LDA with multiple lobes emanating from the steep crater rim, and (2) two separate fluvial valley systems trending towards the crater floor, one from the terminus of the LDA and one from the stippled mantling unit. Vantage point is provided in Figure 1b. Image is CTX P04_002560_2309 draped over MOLA. Scene is ~27 km wide along the crater rim.
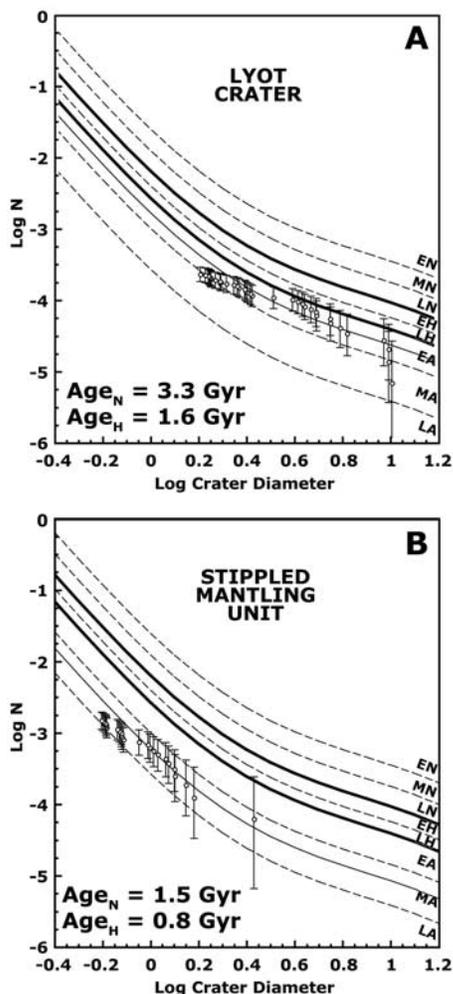
Figure 4. Isochron plots using the Neukum production function [*Ivanov*, 2001] for (a) Lyot Crater and (b) the stippled mantling unit. Valleys incise the stippled mantling unit, thus these data provide a maximum age for the valleys themselves. Best-fit isochrons were calculated for both the Neukum [*Ivanov*, 2001] and Hartmann [*Hartmann*, 2005] systems. Isochrons provide a robust fit to these counts consistent with an Early-Amazonian age for Lyot and a Middle-Amazonian age for the stippled mantling unit. There is a significant (0.8–1.8 Gyr) time span between the Lyot impact and the emplacement of the stippled mantling unit.

[*Ivanov*, 2004] or Martian [*Abramov and Kring*, 2005] environments.

[17] We argue that the unusual climatic conditions in Lyot (low-elevation, high-pressure) are more likely to explain the formation of fluvial valley systems in an otherwise hyper-arid environment. The observed glacial deposits and the stippled mantling unit show that Lyot has been a site of ice-accumulation in the Amazonian, and its low elevation provides pressure above 6.1 mb under present-day conditions [*Haberle et al.*, 2001; *Lobitz et al.*, 2001]. However, the maximum temperature from THEMIS daytime IR data in the vicinity of Lyot is ∼260 K (I03382005).

[18] Thus, for solar insolation to be the energy source to melt ice deposits, a climate different than that observed today is necessary. *Laskar et al.* [2004] have shown that the present obliquity of Mars (∼25.19°) is low and there is an 89.3% probability that the obliquity of Mars surpassed 60° during the last 3 Gyr [*Laskar et al.*, 2004]. Models and GCM simulations [*Mellon and Jakosky*, 1995; *Mischna et al.*, 2003; *Forget et al.*, 2006] argue that during periods of intermediate obliquity (∼35°), the region of water-ice stability and deposition intersects the mid-latitudes and under certain conditions can lead to the formation of extensive glacial deposits. At higher obliquities, models predict increases in temperature at the latitude of Lyot (50°N) [*Mischna et al.*, 2003; *Haberle et al.*, 2003]. At 60° obliquity, *Mischna et al.* [2003] found a maximum diurnally-averaged temperature at 50°N at $L_s = 90$ would be ∼260 K, compared to ∼220 K under current conditions, meaning that peak temperatures would be above 273 K for significant periods of time. Further, *Costard et al.* [2002] calculated that in the southern hemisphere at 50°S on poleward slopes at 45° obliquity, temperatures would exceed 300 K, while daily *average* surface temperatures would exceed 285 K. This thermal wave could melt ground-ice from ∼10−50 cm below the surface [*Costard et al.*, 2002]. The precession cycle may also be important, as an argument of perihelion favoring a warmer northern summer would increase temperatures further. Given these results and the high surface pressure at Lyot caused by its unusual depth, conditions above the triple point are likely to have been achieved after the emplacement of ice-rich units in the Middle/Late Amazonian. Thus, insolation changes from orbital variations are likely to have been a significant energy source for the melting of surface/near-surface ice at Lyot. The interpretation that Lyot was an optimum micro-environment for valley formation is supported by the fact that evidence for melting similar Late Amazonian ice-rich deposits in the mid-latitudes, to the extent observed in Lyot, is not widespread, even though ice remains widely-distributed across these latitudes below a sublimation lag today [*Head et al.*, 2005, 2006a, 2006b; *Holt et al.*, 2008].

5. Summary

[19] Lyot crater represents a unique micro-environment on Mars due to its low elevation and resulting high surface pressure, and its geographic location, which is in a region where glacial deposits are observed and subsurface ice is expected. These factors combined to cause melting of ice-rich deposits to form fluvial valley systems in the interior of the crater. These valleys formed in the Middle to Late Amazonian, significantly post-dating the major period of valley network formation. Chronologically, these valleys are contemporaneous with the glacial deposits and later than the stippled mantling unit that are interpreted to be the source of water (Figures 3 and 4).

[20] A further survey is underway to determine the global extent of young fluvial valley systems in association with Middle and Late Amazonian glacial deposits. The valley systems of Lyot illustrate that fluvial activity occasionally was possible even during the generally cold hyper-arid Amazonian period. These data show that micro-environments permitting liquid water can exist within the context of these conditions, analogous to what occurs today in the Antarctic Dry Valleys [*Marchant and Head*, 2007].

References

Abramov, O., and D. A. Kring (2005), Impact-induced hydrothermal activity on early Mars, *J. Geophys. Res.*, *110*, E12S09, doi:10.1029/2005JE002453.

Bibring, J.-P., et al. (2005), Mars surface diversity as revealed by the OMEGA/Mars Express observations, *Science*, *307*, 1576–1581.

Carr, M. H. (1996), *Water on Mars*, 248 pp., Oxford Univ. Press, New York.

Costard, F., F. Forget, N. Mangold, and J. P. Peulvast (2002), Formation of recent Martian debris flows by melting of near-surface ground ice at high obliquity, *Science*, *295*, 110–113.

Dickson, J., J. W. Head, and D. R. Marchant (2008), Late Amazonian glaciation at the dichotomy boundary on Mars: Evidence for glacial thickness maxima and multiple glacial phases, *Geology*, *36*, 411–414.

Fassett, C. I., and J. W. Head (2008), The timing of Martian valley network activity: Constraints from buffered crater counting, *Icarus*, *195*, 61–89.

Forget, F., R. M. Haberle, F. Montmessin, B. Levrard, and J. W. Head (2006), Formation of glaciers on Mars by atmospheric precipitation at high obliquity, *Science*, *311*, 368–371.

Greeley, R., and J. E. Guest (1987), Geologic map of the eastern equatorial region of Mars, *U. S. Geol. Surv. Misc. Invest. Map, I-1802-B*.

Gulick, V. C., and V. R. Baker (1990), Origin and evolution of valleys on Martian volcanoes, *J. Geophys. Res.*, *95*, 14,325–14,344.

Haberle, R. M., C. P. McKay, J. Schaeffer, N. A. Cabrol, E. A. Grin, A. P. Zent, and R. Quinn (2001), On the possibility of liquid water on present-day Mars, *J. Geophys. Res.*, *106*, 23,317–23,326.

Haberle, R. M., J. R. Murphy, and J. Schaeffer (2003), Orbital change experiments with a Mars general circulation model, *Icarus*, *161*, 66–89.

Hart, S. D., R. A. Parsons, C. J. Barnhart, and V. C. Gulick (2008), Central peak gully formation and morphologies on Mars, *Eos Trans. AGU*, Fall Meet. Suppl., *38*(53), Abstract P41A-1348.

Hartmann, W. K. (2005), Martian cratering 8: Isochron refinement and the chronology of Mars, *Icarus*, *174*, 294–320.

Head, J. W., and D. R. Marchant (2003), Cold-based mountain glaciers on Mars: Western Arsia Mons, *Geology*, *31*, 641–644.

Head, J. W., J. F. Mustard, M. A. Kreslavsky, R. E. Milliken, and D. R. Marchant (2003), Recent ice ages on Mars, *Nature*, *426*, 797–802.

Head, J. W., et al. (2005), Tropical to mid-latitude snow and ice accumulation, flow and glaciation on Mars, *Nature*, *434*, 346–351.

Head, J. W., D. R. Marchant, M. C. Agnew, C. I. Fassett, and M. A. Kreslavsky (2006a), Extensive valley glacier deposits in the northern mid-latitudes of Mars: Evidence for Late Amazonian obliquity-driven climate change, *Earth Planet. Sci. Lett.*, *241*, 663–671.

Head, J. W., A. L. Nahm, D. R. Marchant, and G. Neukum (2006b), Modification of the dichotomy boundary on Mars by Amazonian mid-latitude regional glaciation, *Geophys. Res. Lett.*, *33*, L08S03, doi:10.1029/2005GL024360.

Holt, J. W., et al. (2008), Radar sounding evidence for buried glaciers in the southern mid-latitudes of Mars, *Science*, *322*, 1235–1238.

Ivanov, B. A. (2001), Mars/Moon cratering rate ratio estimates, *Space Sci. Rev.*, *96*, 87–104.

Ivanov, B. A. (2004), Heating of the lithosphere during meteorite cratering, *Sol. Syst. Res.*, *38*, 266–279.

Laskar, J., A. C. M. Correia, M. Gastineau, F. Joutel, B. Levrard, and P. Robutel (2004), Long term evolution and chaotic diffusion of the insolation quantities of Mars, *Icarus*, *170*, 343–364.

Lobitz, B., B. L. Wood, M. M. Averner, and C. P. McKay (2001), Special feature: Use of spacecraft data to derive regions on Mars where liquid water would be stable, *Proc. Natl. Acad. Sci. U. S. A.*, *98*, 2132–2137.

Mangold, N., C. Quantin, V. Ansan, C. Delacourt, and P. Allemand (2004), Evidence for precipitation on Mars from dendritic valleys in the Valles Marineris area, *Science*, *305*, 78–81.

Marchant, D. R., and J. W. Head (2007), Antarctic dry valleys: Microclimate zonation, variable geomorphic processes, and implications for assessing climate change on Mars, *Icarus*, *192*, 187–222.

Mellon, M. T., and B. M. Jakosky (1995), The distribution and behavior of Martian ground ice during past and present epochs, *J. Geophys. Res.*, *100*, 11,781–11,799.

Mischna, M. A., M. I. Richardson, R. J. Wilson, and D. J. McCleese (2003), On the orbital forcing of Martian water and CO_2 cycles: A general circulation model study with simplified volatile schemes, *J. Geophys. Res.*, *108*(E6), 5062, doi:10.1029/2003JE002051.

Mustard, J. F., C. D. Cooper, and M. K. Rifkin (2001), Evidence for recent climate change on Mars from the identification of youthful near-surface ground ice, *Nature*, *412*, 411–414.

————————————

J. L. Dickson, C. I. Fassett and J. W. Head, Department of Geological Sciences, Brown University, Providence, RI 02912, USA. (jdickson@brown.edu)